ARTICLE

Enhance of an efficient sensitivity for the diclhovors detection by a low-weighted gelator based bolaamphiphile amino acid derivatives decorated with a hybrid graphene quantum dots/enzyme/ hydrogel

Received 00th January 20xx,
Accepted 00th January 20xx

DOI: 10.1039/x0xx00000x

Chonticha Sahub[a], Jessica L. Andrews[b], James P. Smith[b], Maya A. Mohamad Arif[b], Boosayarat Tomapatanaget[a*], Jonathan W. Steed[b*]

Going beyond an efficient sensitivity of optical biosensor motivates the exploration of amplification strategy that incorporated the biosensor system in the supramolecular hydrogel. We established the novel fluorescent hybrid materials comprising graphene quantum dots and enzymes supported in L-phenylalanine derived bis(urea) supramolecular hydrogels (**GQDs**/**Enz**/**Gels**) for detection of organophosphate. Addition of acetylcholinesterase (AChE) and choline oxidase (ChOx) during the formation of the self-assembled **GQDs**/**Gel** materials, resulted in enzyme-functionalized gel networks. Significant turn-off fluorescence of the encapsulated **GQDs** in the hydrogels was due to the hydrogen peroxide generated from the active enzymatic reaction. Addition of the insecticide dichlorvos to the **GQDs/Enz/Gels** materials resulted in the recovery of the fluorescence in proportion to the concentration of dichlorvos, with a detection limit of 2.61×10^{-8} M which outperforms analogous in solution by 100-fold improvement and a wider linear range of 1.25×10^{-8} – 1.25×10^{-4} M compared to biosensor in solution. These hybrid hydrogels show promising sensitivity for detection of oxy-form organophosphate pesticide and expectedly offer scope for the development of rapid and environmentally friendly techniques.

Introduction

Supramolecular, or low molecular weight gels, and particularly hydrogels, have wide ranging applications in areas such as controlled drug release[1-2], enzyme stabilization and immobilization[3-5], pharmaceutical polymorph control [6-8], anion or metal ion sensing [9-13], and as biosensors [14-16]. Supramolecular hydrogels arise from the self-assembly of low molecular weight gelators (LMWG) and large amount of water (typically higher than 99% by mass) using non-covalent interactions. Bolaamphiphilic molecules comprise of at least two parts including a hydrophobic skeleton such as alkyl chains, a steroid, or a porphyrin and two hydrophilic groups on both ends which are symmetric or asymmetric end group. Most bolaamphiphiles with the hydrophobic spacers have been designed as low molecular mass gelators[17-19] which is a technical advantage in terms of the low concentration required for formation of aqueous or organic gels. For gel formation, the interaction between bolaamphiphilic based gelator stemmed from the hydrogen bonds, hydrophobic effect, π–π stacking interaction. These noncovalent interactions of bolas can form self-assemble to generate the sheets, micelles, vesicle, fibers and nanotubes. [20-22] Work of Minghua Liu[23] demonstrated the novel bolaamphiphilic gelators with L-glutamic acid as end group, connecting with the rigid aromatic substituents by varying the different lengths of alkyl chains as spacers which greatly changes the gelation property and the gel structures. Particularly, the even-odd alkyl chain would influence to the gelating and self-assembly under the hydrogen bonding from amide groups and a strong π–π stacking interaction. Arindam Banerjee[24] reported the metal-ion-induced, pH-responsive hydrogel formation using phenylalanine-based bolaamphiphilic molecule. One of these metallo-hydrogels showed a benefit for encapsulation of vitamin B12 molecules with slowly releasing under various pH system. Moreover, there are the research presenting that inorganic silica gel and gold particles exhibited much more stable under an organic Bolaamphiphilic molecules monolayer. A technical advantage of the Bolaamphiphilic molecules is attractive in terms of the low concentration at which aqueous or organic gels are formed[25]. Non-chemically crosslinked hydrogels have been extensively studied in the context of enzyme encapsulation and stabilization[3]. However, a flexible and porous structure is required to facilitate full penetration of the enzyme into the substrate and therefore, solid-phase substrates such as metal nanoparticles, or even a mobile gel-type networks without well-defined pores, have seen less success[26-28]. Hence, the immobilization of amphiphilic GQDs and enzymes into hydrogels remains of great interests for amplifying a signal to give high sensitivity for sensing applications and maintaining enzymatic activity in biological applications. Considerably, carbon dots mediated through the hydrogel encapsulation show advantageously in high fluorescent intensity compared to those in solution.[29-30] Its benefit of high sensitivity for sensing application is of great merits.

[a] *Address here.*
[b] *Address here.*
[c] *Address here.*
† Footnotes relating to the title and/or authors should appear here.
Electronic Supplementary Information (ESI) available: [details of any supplementary information available should be included here]. See DOI: 10.1039/x0xx00000x

Organophosphate pesticides (OPs) such as dichlorvos, paraoxon and parathion are insecticides used worldwide in the agricultural industry. Several organophosphate pesticides can directly disturb the active site of acetylcholinesterase (AChE) enzyme in the insect's nervous system subsequently leading to insect death[31-32]**.** However, they can also persist as contaminants in food, soil, water, and the environment, which can seriously impact human health.[33-36]

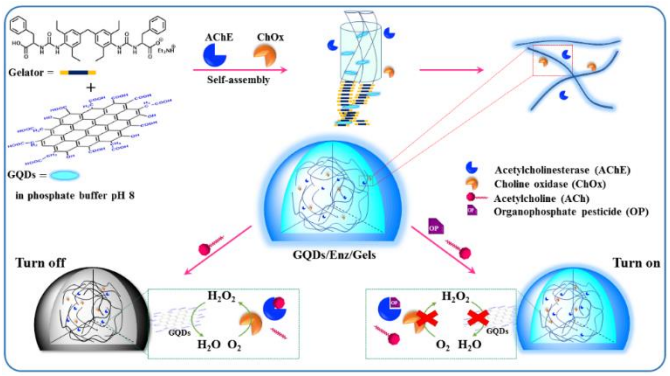

Scheme 1. Hybrid hydrogels of **GQDs/Enz/Gels** and proposed mechanism of organophosphate pesticide detection.

In our previous work, we have reported the determination of organophosphate pesticides by using GQDs in the solution phase under an enzymatic reaction[37]. However, the requirement of materials for highly sensitive and easy to engineer as a sensing device for the detection of organophosphate pesticides remains.

In this work, we have constructed a highly sensitive and convenient organophosphate sensing system based on a hybrid hydrogel system integrating GQDs, enzymes and small molecule hydrogelators to selectively detect organophosphate with extremely high sensitivity. The design incorporates bolaamphiphile gelators based on bis(urea)s and amino acid derivatives. These functionalities impart compatibility with the water-soluble double-enzyme system (AChE and ChOx) in phosphate buffer. Bis(urea) derivatives are an effective supramolecular gelators because their hydrogen-bonded α-tape motif promotes one-dimensional fibril formation in conjunction with hydrophobic and π-stacking interactions[38-40]. Quantitative analysis of OPs using this hybrid material arises from the turn-on PL response observed in the presence of the pesticide and is caused by inhibition of the enzymatic production of hydrogen peroxide, which quenches luminescence as shown in Scheme 1. To the best of our knowledge, this hybrid hydrogel material is the first fluorescent hydrogel probe integrating **GQDs** and enzymes with a small-molecular gelator. Fantastically, this system gives extremely high sensitivity, down to nanomolar levels of detection.

Results and Discussion

Synthesis and characterization of hybrid hydrogel materials

In the present work we have screened a range of bolaamphiphile moiety, amino acid derived gelators with hydrophobic central spacers. The structures are based on tetraethyldiphenyl methane (compounds **1**-**4**) and bis(methylethyl)benzene linkers (compound **5**-**6**), with a chemically diverse range of end groups derived from biocompatible amino acids, including L-valine methyl ester (**1**), L-phenylalanine methyl ester (**3** and **5**), L-leucine (**2c**); and L-phenylalanine (**4a-c** and **6a-b**). Depending on the pH, these gelators exist either as the free acids, or as singly or doubly deprotonated forms. Free acids are denoted with the 'a' suffix, singly deprotonated species as 'b' and doubly deprotonated as 'c'. The molecular structures of all gelators are shown in Fig. 1. The synthesis of all compounds was achieved *via* a one-step reaction of the precursor diisocyanate and the requisite amino acid derivatives in the presence of triethylamine. With the characterization of all gelators, the ^{1}H NMR spectra and analytical data are sensitive to the protonation state and the representative ^{1}H NMR spectra for compounds **4a**, **4b** and **4c** are shown in the supporting information, Fig. S8. The

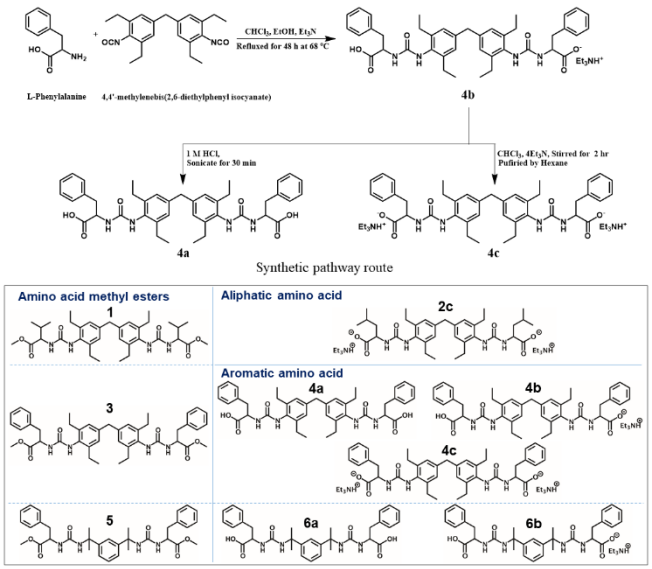

assignment of the acidic OH and NH resonances was confirmed by D_2O exchange.

Fig 1. Synthetic pathway route of gelators **4b**, **4a** and **4c**, and molecular structures of gelators **1**-**6b** based on bis(urea) and amino acid derivatives

The gelation behavior of all compounds was tested in various solvents as shown in Tables **S1** – **S9**. They were found that the sterically bulky bis(methylethyl)benzene spacer group (**5**, **6a** and **6b**)[41] did not form gels in any solvents and compounds with the tetraethyl diphenylmethane spacer (**1**, **3**, **4a**, **4b** and **4c**), showed good gelation behavior in many solvents at 1 wt%, especially for **4b** in Fig. S9. For enzyme compatibility, the gelation in water to form hydrogels is of key importance, particularly since the target organophosphate analytes are also water soluble. Moreover, previous work by our group[42] reported that carbon dots encourage hydrogel formation. Hence, we investigated hybrid hydrogel formation of each gelator in conjunction with GQDs in water (Table S10). Gel formation in water was observed for compounds **4b** and **4a** within 5 min, in contrast to the same system in the absence of GQDs. To facilitate organophosphate detection *via* an enzymatic reaction, the enzymes must be immobilized in the hybrid hydrogel. Therefore, we attempt to retard the hydrogel formation to facilitate penetration of the enzyme into the gel matrix. As expectation, decreasing the gelator concentration to 0.25 – 0.5%wt resulted in increasing the hydrogel formation time. From Table S10 showing the

gel formation of all gelators, it was found that the gel formation by **4b** in water was found to take 30 min, while **4a** exhibited a gel formation time of 4 h under these conditions.

Focusing on **4b**, the gelation behavior was studied at 0.3-1 wt% by increasing the concentration of **GQDs** from 0-3 mg/ml (Table S11 and Fig. S12). The data showed that the gelator preferentially formed the hybrid gel in the presence of **GQDs**. Gelation for the mono-deprotonated **4b** was observed within 30 minutes in the presence of 2 and 3 mg/ml of GQDs at 0.5 wt% gelator. In contrast to pure water, gelation of phosphate buffer solution at pH 8 proved to be significantly more efficient with **4b** forming gels at 2 wt% after 30 min even in the absence of **GQDs**.

The mechanism by which the **GQDs** enhance gelation is not clear, however it may result from additional cross-linking of the gel fibrils by adsorption of the **GQDs** onto the hydrophobic surface of the gel fibril. The dominant driving force for gel fibril assembly is the hydrophobic interaction[43] . We postulate that **GQDs** interact with the gelators *via* π-π stacking between the hydrophobic spacer or aromatic residue of the phenylalanine substituent, and hydrogen bonding between the terminal carboxylate of the amino acid and the GQD peripheral groups resulting in an enhanced hydrogel formation [44].

Since enzyme activity is usually affected by the pH condition, thus,pH and buffer concentration should be investigated in this sensing system. The gelation behavior of **4a** – **4c** integrated with GQDs was therefore examined at pH of 6 – 9 in different concentration of phosphate buffer collected in Table S12. In general, the pH changes in 6-9 range showed similar gelation behavior. However, our previous work reported the efficient activity of enzyme at pH 8. Hence, the dependence on buffer concentration at pH 8.0, thus, was examined from 10 – 50 mM of phosphate buffer solution. Surprisingly, complete hydrogel formation was observed at 25 and 50 mM of buffer solution, both with and without **GQDs** (Table S13). Considering in Fig. 2A, gel formation without **GQDs** was also observed within 30 min, at 0.5wt% of **4a** and **4b** in 25 – 50 mM phosphate buffer, at pH 8.0. However, regards of the optimal **GQD** hybrid gel formation is shown in Fig. 2(C–D), indicating that 0.5 wt% of **4b**, combined with **GQDs** showed a well-formed hydrogel and transparent gels in 10 and 25 mM phosphate buffer solution pH 8.0.

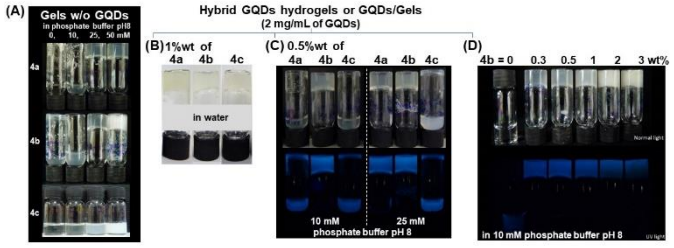

Fig 2 Photographs of gel behavior at 30 min (A) gel formation studies of gelators **4a**, **4b** and **4c** without **GQDs** in various concentration of phosphate buffer pH 8; the **GQDs/Gels** from (B) 1wt% gelators **4a**, **4b** and **4c** in water; the **GQDs/Gels** under (C) different concentration of phosphate buffer and (D) different wt% of gelator **4b**, respectively.

These results show that the mono-deprotonated compound **4b** forms significantly more robust hydrogels than either the free acid or doubly deprotonated form, compounds **4a** and **4c,** respectively. Moreover, the concentration of the gelator **4b** in 10 mM phosphate buffer pH 8 was studied over the range of 0–3 wt% as Fig. 2D. Transparent hybrid **GQDs/Gels** were obtained at concentrations of 0.3 and 0.5 wt% of **4b** in the presence of 2 mg/ml of **GQDs** and 10 mM phosphate buffer at pH 8. These conditions produced gels with optimum properties and were therefore chosen for further photoluminescent (PL) sensing studies.

The formation of the gels and their bulk mechanical properties were examined by frequency and stress sweep rheometry. The rheological properties of gels of compound **4b**, both with and without **GQDs**, in both water and phosphate buffer at pH 8, are shown in Figs. 3A and B. Only very weak partial gels are formed from 0.5wt% of gelator **4b** in water. Gelation can, however, be enhanced by the addition of **GQDs** or by using phosphate buffer as the solvent, as shown by the larger *G´*values shown in Table 1.

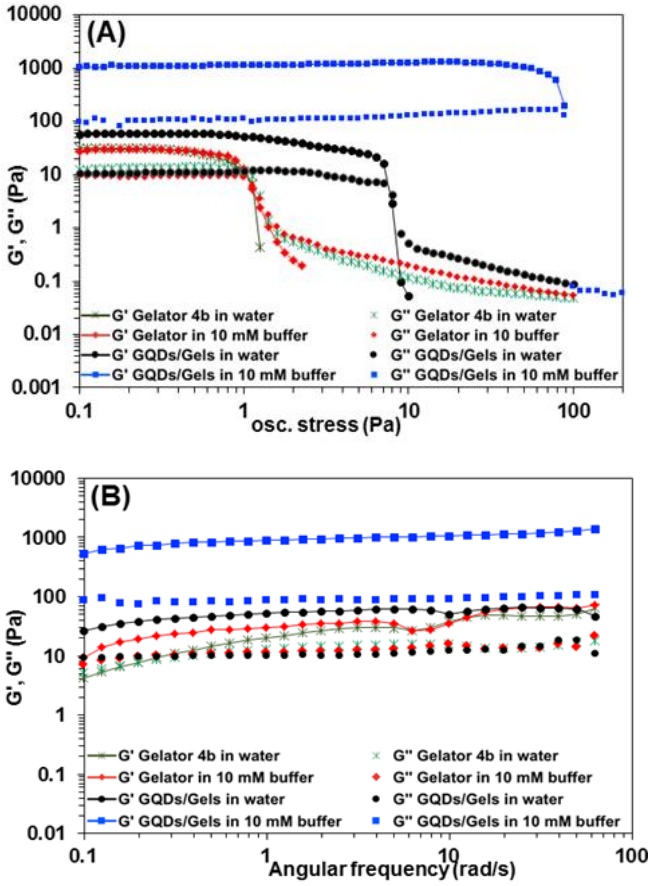

Fig. 3. (A) Stress sweep and (B) frequency-sweep rheology of gelator **4b** and **GQDs/Gels** from **4b** in different conditions.

Under optimized conditions, gels of compound **4b** produce *G'* values up to 1100 Pa and yield stresses up to 100 Pa. These results are consistent with the visual observation that the gels of **4b** containing **GQDs** and phosphate buffer are relatively robust.

Table 1 Summarized values of storage modulus and loss modulus of samples in various conditions

Gelator	GQDs (mg/ml)	PB buffer (mM)	Storage modulus, G′ (Pa)	Loss modulus, G′′(Pa)
4b	-	0	30±2	14±1
4b	-	10	28±1	9±0.2
4b	2	0	60±1	11±0.3
4b	2	10	1160±75	112±14

Preparation of hybrid GQDs/Enz/Gel materials

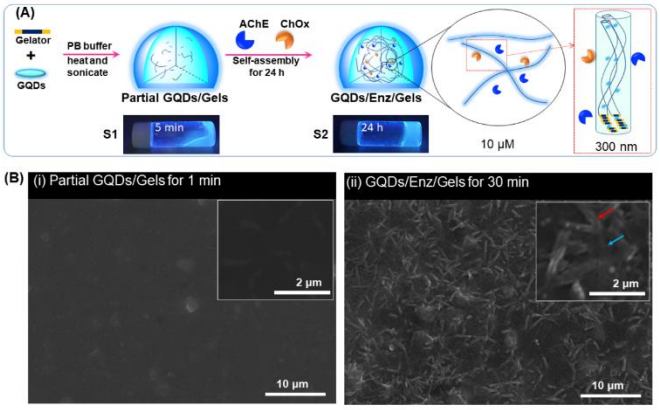

Fig 4. (A) Preparation of partial **GQDs/Gels** (stage1) and **GQDs/Enz/Gels** hybrid hydrogels (stage2). (B) SEM images of the dried partial gels (xerogels) from stage 1 prepared for 1 min and the hybrid hydrogels from stage 2 prepared for 30 min followed by drying under ambient conditions for 2 days.

The enzyme-loaded PL sensing hybrid gel materials (**GQD/Enz/Gel**) were prepared in two stages (S1 – S2) as shown in Fig 4A and the methodology preparation was explained in supporting information (Figs. S14-15). The microstructure of the dried (xerogel) stage 2 materials was examined by SEM. Gels prepared from compound **4b** in 10 mM phosphate buffer showed a relatively featureless SEM image comprising spots which are likely to be buffer, and isolated fibers with average diameter of 200 nm as shown in Fig. S16. In the case of the **GQDs/Gels** formed for 1 min, the SEM image of the xerogel (Fig 4B) exhibited short, fibrous particles with an average diameter of 290 nm. Well-defined supramolecular networks of **GQDs/Enz/Gels** were found 30 min after initial gelation, in the presence of the enzymes, and the inset shows the longer, fibrous networks, which were additionally surrounded by many small fibers with average diameter of 50 nm (blue arrow).

It is likely that the small fibers gradually self-assemble with **GQDs** to form hybrid supramolecular networks *via* hydrophobic, π-π stacking and hydrogen bonding interactions. The hydrophilic enzymes are likely to be trapped inside the aqueous pores or on the surface of the hydrophobic gel fibers, which allows them to retain their activity[15, 44]. The **GQDs** are typically less than 10 nm in size and, therefore, could not be observed by SEM. [37]

The ATR-FTIR spectra of the xerogels of the hybrid **GQDs/Enz/Gel** materials comprising a combination of **GQDs**, enzymes and gelator **4b** are also examined to confirm the **GQD** and Enz encapsulated in Gel as shown in Fig. S17. The spectra of these hybrid materials show a board absorption band at 3000-3500 cm^{-1} (NH and OH stretch), and peaks at 1633-1645 cm^{-1} (ν_{CO} and ν_{CN} of amide I of enzymes), 1574 cm^{-1} (ν_{asCOO^-} of **GQDs**), 1574-1496 (δ_{NH} and ν_{CN} of urea in gelator **4b** and amide II of enzymes)[45-46] as well as 1386 cm^{-1} (ν_{sCOO^-}) and 1077 cm^{-1} ($\nu_{C\text{-}OH}$)[47], belonging to the characteristic peak of -COOH and -OH groups of the edge of **GQDs**, respectively. Additionally, the appearance of a small peak at 1641 cm^{-1} and the peak at 1574 cm^{-1} are indicative of an amide I and amide II, respectively, of the enzyme backbone[45-46]. The low intensity of peaks assigned to the enzymes is likely to be caused by their very low concentration compared to the **GQDs** and gelator **4b** in these materials. The spectra of these hybrid materials showed characteristic peaks corresponding to the gelator, enzymes and edge functionalities of the **GQDs**[48-49]. Further information can be found in the supporting information.

Responses of hybrid GQDs/Enz/Gels to H_2O_2 generated in situ

Based on our previous work[37], H_2O_2, generated from the active enzymatic reaction of acetylcholinesterase and choline oxidase, can react with **GQDs**, resulting in a *"*turn-off*"* fluorescence of **GQDs**. Regarding to a well-known H_2O_2 behavior in the peroxidase-like catalytic activity, the H_2O_2-responsive behavior of the hybrid **GQDs/Gels** was investigated by following their photoluminescence intensity at 465 nm. As the results in Fig. S18 at 60 min after the H_2O_2 addition, the luminescence of hybrid **GQDs/Gels** containing 0.5 wt% of **4b** was quenched significantly in the presence of peroxide. This implies facile penetration of H_2O_2 through these relatively weak gels which facilitates a strong PL response. This analysis reveals that the fluorescence quenching is proportional to the concentration of H_2O_2. To verify the PL response properties sensing materials, the compared PL responses of **GQDs**, **GQDs/Gels**, and **GQDs/Enz/Gels** systems have been investigated. It was found that an incorporation of the enzymes into the **GQDs/Gels** resulted in a PL intensity higher than the **GQDs** without gels as displayed Fig B. Hence, the enhanced PL intensity of the hybrid hydrogels is likely to stem from the stabilizing interaction between gelators and **GQDs** and hydrophobic surface of the gel fiber. Interestingly, the PL quenching of the **GQDs/Enz/Gels** hybrid materials upon adding acetylcholine (stage 3, S3) is highly dependent on the enzymatic reaction occurring within the gel. The acetylcholine is hydrolyzed by AChE and ChOx to generate H_2O_2, which quenches the PL intensity as in Fig. 5B (orange line). The observed quenching behavior confirms the enzymes which have been encapsulated into the hybrid hydrogels and corresponds to the schematic illustration in Fig.5A.

Stability of enzyme-based materials under mild conditions between 5 – 37 °C is of considerable importance, particularly in countries such as Thailand where ambient temperatures can routinely reach 37 °C. The relative enzyme activities in both the gel and aqueous phase were compared over a range of temperatures, by monitoring the PL quenching, Fig.5C. At 5 °C, the relative enzyme activity (%) in both systems is similar to the control. The activity of materials stored at room temperature (25 °C) was slightly decreased

and was significantly reduced upon storage at 37 °C. Interestingly, the activity of the enzyme after incubation in the gel phase for 4h at 37 °C (> 50% of relative enzymatic activity remained) were much greater than that in aqueous solution (< 10% of relative enzymatic activity remained). These results suggest that hydrogels obtained from gelator **4b** can significantly stabilize the enzyme activity. Furthermore, the activity of the **GQDs/Enz/Gels** remained at more than 90 % upon storing at 5 °C for 15 days, as shown in Fig. S20. This implies that the gelator **4b** stabilizes the single sheet **GQDs** and prevents aggregation[42, 50].

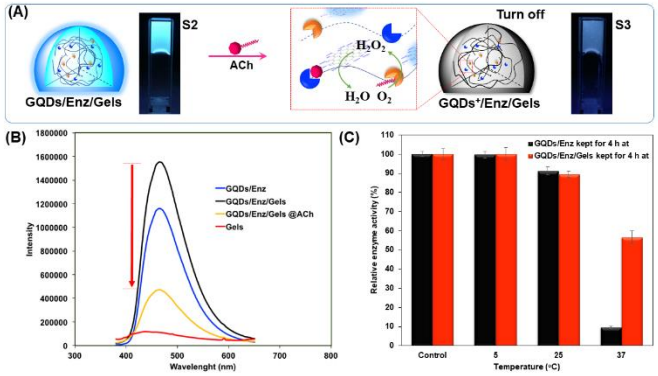

Fig 5. (A) Scheme of H_2O_2-responsive in situ **GQDs/Enz/Gels** biosensor (stage 3). (B) The PL quenching of biosensor after adding acetylcholine. (C) In comparison of relative enzyme activity between in aqueous solution and gel phase after incubated in 5, 25 and 37 °C for 4 h.

Concentration of enzyme for the responsive sensing

Optimized conditions including the temperature, pH and concentration of enzymes and acetylcholine are all necessary for OP detection and the results were exhibited in Fig. S22. For all tests, the hybrid hydrogel (**GQDs/Gel**) in the partially gelled state was incubated with ACh for 20 min, prior to PL measurement. A comparison of the normalized PL intensity of **GQDs/Gels** and **GQDs/Enz/Gels** after incubation with ACh for 20 min was shown in Fig S22. Introduction of the enzymes AChE and ChOx at 2.5 U/mL and 0.625 U/mL, respectively, resulted in significant PL quenching of the **GQDs/Enz/Gels** system. Interestingly, the PL quenching of the **GQDs/Enz/Gels** increased upon increasing the concentration of both enzymes, with a 5 mM concentration of ACh providing the most significant PL quenching. Compared to the PL quenching of the enzyme-free **GQDs/Gel** system, the **GQDs/Enz/Gel** showed a remarked increase of PL quenching upon addition of ACh. However, higher concentrations of ACh (7.5 and 10 mM) showed lower PL quenching. This observation is rationalized by direct interference of ACh with the **GQDs** in the hybrid materials, even in the absence of an enzyme. The optimal conditions for sensing proved to be 12.5 mM phosphate buffer pH 8, at 37 °C. This allowed optimal activity of the AChE and ChOx enzymes for acetylcholine hydrolysis, consistent with previous works[51-54]. To minimize the cost-efficiency of the sensor, low concentrations of enzyme at 2.5 U/mL of AChE, and 0.625 U/mL of ChOx were employed for our sensing studies.

Organophosphate Sensing study

Related to our concept, the proposed mechanism for OP detection is illustrated in **Error! Reference source not found.**6A. AChE catalyzes the hydrolysis of acetylcholine (ACh) to produce choline that can be continuously oxidized by ChOx to generate H_2O_2 and result in PL quenching of the hybrid gels. OPs preferentially bind to the active site of AChE[32], thereby deactivating the enzyme and consequently inhibiting H_2O_2 generation. Consequently, recovery of the PL response was observed. Gratifyingly, the visual changes showed that the PL intensity of **GQDs/Enz/Gels** depended on the concentration of dichlorvos, which inhibited the activity of AChE in the hybrid hydrogels (Fig 6B). Other OPs including, parathion, malathion, and methyl-paraoxon at concentrations of 1.25 and 12.5 μM were also examined for the inhibition efficiency (I%) of AchE. Inhibition efficiency was calculated *via* equation S1 in SI.

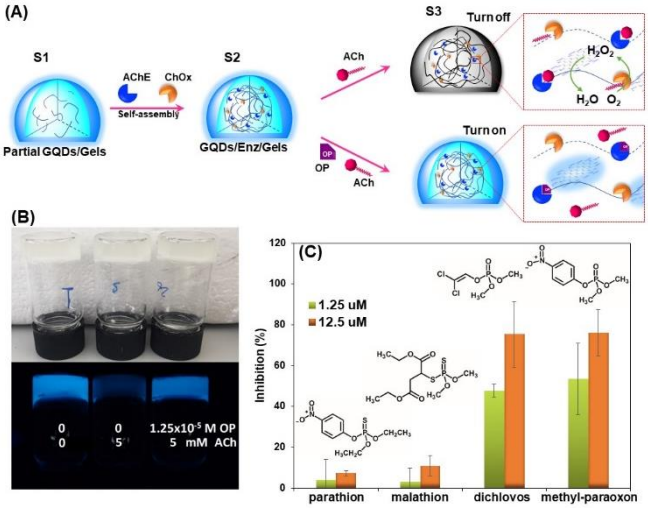

Fig 6. (A) Proposed mechanism of hybrid **GQDs/Enz/Gels** for organophosphate pesticide detection. (B) visual changes of **GQDs/Enz/Gels** with various amount of OPs and ACh. C) Comparison of inhibition efficiency (%) of AChE in hybrid hydrogels after incubation in 1.25 x10^{-6} and 12.5 x10^{-6} M of four organophosphate pesticides.

From Fig. 6C, the inhibition efficiency (I%) and hence PL recovery at two concentrations showed a similar trend for both methyl-paraoxon and dichlorvos, which are higher than malathion and parathion, respectively. The inhibition efficiency of AChE by OPs in oxo-form of the phosphate group are higher than that of OPs in thio-form, possibly caused by tighter binding of the oxo-form to the enzyme[55-56]. Therefore, we further studied the sensing ability of **GQDs/Enz/Gel** toward the oxo-functionalized pesticides, dichlorvos and methyl-paraoxon.

The PL inhibition of the **GQDs/Enz/Gel** hybrid system showed an excellent correlation with the concentration of OPs. A calibration curve is shown in Figs. 7A and 7B. The inhibition efficiency (%I) of AChE towards dichlorvos (DV) and methyl-paraoxon (MP) exhibits a linear range of 1.25x10^{-8} to 1.25x10^{-4} M and 1.25x10^{-9} to 0.625x10^{-4} M, respectively, which represent considerably better linearity than our previous work[37]. Most sensing systems based on enzymatic reactions show a pesticide-detection limit of 10% inhibition of AChE[56]. Importantly, the limits of detection (LOD) of this hybrid material towards DV and MP are 2.61x10^{-8} M and 6.79x10^{-9} M,

respectively, more than two orders of magnitude compared to our previous work without a supramolecular gel component[37].

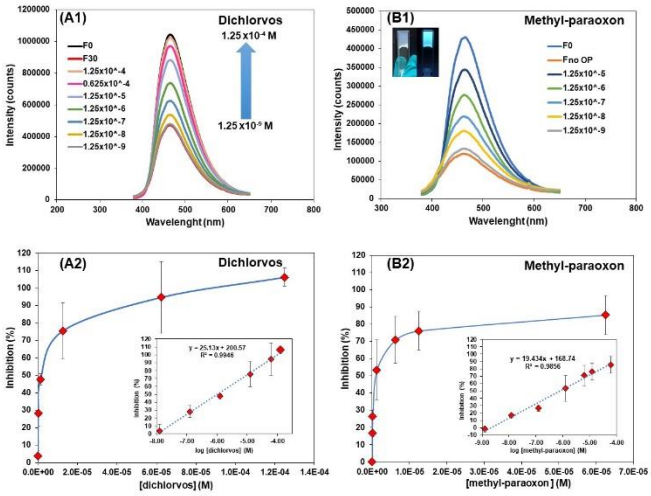

Fig 7. PL emission intensity and calibration curves of **GQDs/Enz/Gels** upon the increasing of dichlorvos (A) and Methyl-paraoxon concentration (B) between 1.25x10^{-9} to 1.25x10^{-4} M (λ_{ex} = 360 nm).

Moreover, the detection of organophosphate in the literature reviews was compared in Table 2. It was found that our material offers the efficacy of sensitivity for detection of OPs especially, dichlorvos and methyl-paraoxon.

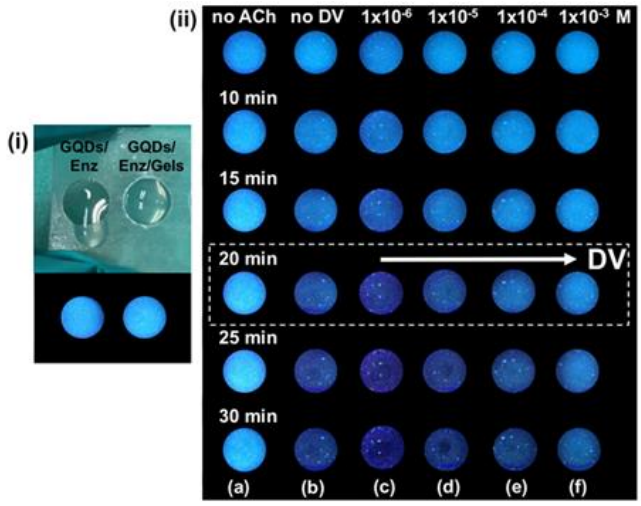

Fig 8. Photographs of hybrid **GQDs/Enz/Gels** sensory chips (Glass slide 7.6 x 2.6 cm and circle with diameter of 0.5 cm) in the presence of various concentration of dichlorvos (DV) and time of measurement.

Table 2. The comparison of linear range and LOD between this work and previous works.

Organophosphate	Sensing methods	Linear range (μM)	LOD (μM)	Ref.
dichlorvos	Amperometric	Not reported	3.62x10^3	57
	Visual screening card	Not reported	0.45	58 52
	Optical mode	2.26-31.67	2.26	59
	Spectrophotometric	0.45-45	0.78	31
	Spectrophotometric	0.0125-125	0.0261	This work
paraoxon	Fiber optic	10-500	2	60
methyl-paraoxon	Square wave voltammetric	0.5–100	0.24	61
	Spectrophotometric	Not reported	6.18 x 10^3	62
	Spectrophotometric	0.40-40	0.34	31
	Spectrophotometric	0.00125-62.5	0.00679	This work

The development of a small scale, rapid, convenient, and high-throughput sensing system for OPs is currently of increasing interest. A portable lab comprising a small-scale hybrid hydrogel on a glass slide was prepared as a method of screening for dichlorvos in Fig. 8. The naked-eye fluorescence images obtained by the **GQDs/Enz/Gels** with dichlorvos, under UV irradiation at 365 nm displayed a significant brightness change upon increasing the analyte concentration from 1x10^{-6} to 1x10^{-3} M. After the system was exposed to ACh for 20 min, the RGB value was evaluated using imageJ software[63], which showed a particular increase in the green values as a function of DV concentration (Fig S23). These results suggest that the **GQDs/Enz/Gels** system proposed in this work is suitable for development as a convenient sensor for OPs, offering a rapid and extremely sensitive readout, for further expected applications in food, water and the environment.

Conclusions

We have developed a new low molecular weight, bis-urea gelator (LMWG), comprising a diphenylmethane spacer and phenylalanine end groups, which forms robust gels in phosphate buffer, when combined with graphene quantum dots (**GQDs**). The use of phosphate buffer as a solvent is easily accessible and highly

compatible with biological systems.[64-66] The enzymes AChE and ChOx can be incorporated in the GQD-containing hydrogel as a signaling unit, without loss of activity. The resulting **GQDs/Enz/Gels** hybrid material acts as a highly effective turn-on sensor for the detection of organophosphate pesticides. In comparison to the analogous aqueous system, the hybrid gel material exhibits markedly improved linear range, sensitivity, and stability. The hybrid hydrogel material showed 10-100-fold improvement in the limit of detection (LOD) and linearity range, compared to the analogous enzymatic reaction by **GQDs/Enz** in solution. This work also provides new insight into improving the performance of low molecular weight hybrid hydrogels through combination with **GQDs** and phosphate buffer. The result is a highly effective and potentially versatile sensing system, with a high sensitivity and stability. To our knowledge this is the candidate sensing system regarding to the enzymatic turn-on sensing in a small molecule gel medium.

Experimental Section

All gelators (Figs. S1-S7) and **GQDs** were synthesized, and then gel formations were studied in various solvents as shown in Supporting Information.

Graphene Quantum Dots

Graphene quantum dots were prepared according to Dong's method.[47] Citric acid (2 g, 0.01 mol) was heated to 200 °C for 30 min and the resulting liquid GQDs were added dropwise to 100 mL NaOH solution (10 mg/mL^{-1}) under vigorous stirring. The pH was adjusted to 8.0 by addition of 1 M HCl solution, and the product was then isolated by dialysis 2,000 Da**.**

Gel Screening Procedure

The gelation behavior of each gelator was examined in several solvents with different polarities including water, ethanol (EtOH), methanol (MeOH), 1-propanol, acetone, dimethyl sulfoxide (DMSO), chloroform, hexane, cyclohexane and cyclohexanone. 0.5 mL of each solvent was added to 5 mg (1% wt) of each gelator in a sealed vial. The mixture was sonicated for 30 sec, and then heated for 30 seconds. Gel formation was identified by the inversion test.

Preparation of Hybrid GQDs/Gels and GQDs/Enz/Gels

The **GQDs/Gels** was prepared by following method. **GQDs** solution and phosphate buffer (1 mL of mixed solution comprising 2 mg/ml of **GQDs** and 10 mM of phosphate buffer solution) was added to 5 mg of gelator **4b** (0.5% wt) in a sealed vial. Then the suspension was sonicated for 30 seconds and then heated for 30 sec until the solid had dissolved. After 5 min, 0.1 mL of acetylcholinesterase (AChE) and 0.1 mL choline oxidase (ChOx) were added to the partial gels and the mixture was left at 5 °C for 24 h to form the hybrid hydrogel part of the **GQDs/Enz/Gels** biosensor.

The Determination of Organophosphate Pesticides

The hybrid **GQDs/Enz/Gels** were used to determine the concentration of organophosphate pesticides (OPs) by monitoring the photoluminescence intensity of the system at 465 nm, after the addition of the OPs. Firstly, 0.2 mL of an OP solution at a range of concentrations was added to 1.2 mL of **GQDs/Enz/Gels** in a sealed vial and incubated at 37 °C for 15 min. 0.2 mL of 40 mM of acetylcholine (ACh) was then added to the sample and the mixture was incubated at 37 °C for a further 20 min. The sample was transferred to a cuvette and PL intensity at 465 nm was measured using the same method as in the H_2O_2-response studies. Each experiment was repeated 3 times. The **GQDs/Enz/Gels** were studied using the final concentrations of 1.25 mg/ml of GQDs, 1.25 U/mL of AChE, 0.3125 U/mL of ChOx and 0.3125 %wt of **4b** in 12.5 mM phosphate buffer.

Scanning Electron Microscopy

The **GQDs/Gels** and **GQDs/Enz/Gels** samples were prepared and cooled at room temperature for 1 and 30 min, respectively, then dropped onto a glass slide and dried in air, at room temperature for 2 days. The samples were coated with Au ions and imaged using a JSM-IT 100 scanning electron microscope. The average diameter of the gel fibers was obtained by measuring 100 fibers per SEM image using ImageJ software (ImageJ 1.49 V free software with Java 1.6.0 65(32-bit) obtained from https://imagej. nih.gov/ij/, Wayne Rasband, National Institutes of Health, USA).

Conflicts of interest

There are no conflicts to declare.

Acknowledgements

The project was funded by the Thailand Research Fund (RSA6080012) and National Research Council of Thailand (NRCT): NRCT5-RSA63001-23). The authors would like to acknowledge Durham University, UK and Chulalongkorn University, Thailand for facility support and funding the project. CS is a Ph.D. student supported by the Development and Promotion of Science and Technology Talent Projects (DPST). We also thank the UK Engineering and Physical Sciences Research Council for studentship support (JPS) and funding *via* the Soft Matter and Functional Interfaces Centre for Doctoral Training (JLA).

Notes and references

1. Y. Li, F. Wang and H. Cui, Peptide-Based Supramolecular Hydrogels for Delivery of Biologics, *Bioeng. Trans.l Med*., 2016, **1**, 306-322.

2. R. Ravichandran, M. Griffith and J. Phopase, Applications of self-assembling peptide scaffolds in regenerative medicine: the way to the clinic, *J. Mater.Chem. B*., 2014, **2**, 8466-8478.

3. H. Liang, S. Jiang, Q. Yuan, G. Li, F. Wang, Z. Zhang and J. Liu, Co-immobilization of multiple enzymes by metal coordinated nucleotide hydrogel nanofibers: improved stability and an enzyme cascade for glucose detection, *Nanoscale*, 2016, **8**, 6071-6078.

4. L.S. Moreira Teixeira, J. Feijen, C.A. van Blitterswijk, P.J. Dijkstra and M. Karperien, Enzyme-catalyzed crosslinkable hydrogels: Emerging strategies for tissue engineering, *Biomaterials*, 2012, **33**, 1281-1290.

5. H. Shigemitsu, T. Fujisaku, S. Onogi, T. Yoshii, M. Ikeda and I. Hamachi, Preparation of supramolecular hydrogel–enzyme hybrids exhibiting biomolecule-responsive gel degradation, *Nat. Protoc*., 2016, **11**, 1744.

6. M. Pauchet, T. Morelli, S. Coste, J.-J. Malandain and G. Coquerel, Crystallization of (()-Modafinil in Gel: Access to Form I, Form III, and Twins, *Cryst. Growth Des*., 2006, **6**, 1881-1839.

7 L. Kaufmann, S.R. Kennedy, C. D. Jones and J. W. Steed, Cavity-containing supramolecular gels as a crystallization tool for hydrophobic pharmaceuticals, *Chem. Commun*., 2016, **52**, 10113-10116.

8 C. Ruiz-Palomero, S.R. Kennedy, M.L. Soriano, C.D. Jones, M. Valcarcel and J.W. Steed, Pharmaceutical crystallization with nanocellulose organogels, *Chem. Commun*., 2016, **52**, 7782-7785.

9 J.A. Foster, R.M. Edkins, G.J. Cameron, N. Colgin, K. Fucke, S. Ridgeway, A. G. Crawford, T. B. Marder, A. Beeby, S. L. Cobb and J. W. Steed, Blending Gelators to Tune Gel Structure and Probe Anion-Induced Disassembly, *Chem. Eur. J*., 2014, **20**, 279-291.

10. J.A. Foster, M.O. Piepenbrock, G.O. Lloyd, N. Clarke, J.A. Howard and J.W. Steed, Anion-switchable supramolecular gels for controlling pharmaceutical crystal growth, *Nat. Chem*., 2010, **2**, 1037-1043.

11. L. Meazza, J.A. Foster, K. Fucke, P. Metrangolo, G. Resnati and J.W. Steed, Halogen-bonding-triggered supramolecular gel formation, *Nat. Chem.,* 2013, **5**, 42-47.

12. C.A. Offiler, C.D. Jones and J.W. Steed, Metal 'turn-off', anion 'turn-on' gelation cascade in pyridinylmethyl ureas, *Chem. Commun*., 2017, **53**, 2024-2027.

13 M.O. Piepenbrock, G.O. Lloyd, N. Clarke and J.W. Steed, Metal- and anion-binding supramolecular gels, *Chem. Rev.*, 2010, **110**, 1960-2004.

14 M. Ikeda, T. Tanida, T. Yoshii, K. Kurotani, S. Onogi, K. Urayama and I. Hamachi, Installing logic-gate responses to a variety of biological substances in supramolecular hydrogel-enzyme hybrids, *Nat Chem*, 2014, **6**, 511-518.

15 A. Wada, S.-i. Tamaru, M. Ikeda and I. Hamachi, MCM−Enzyme−Supramolecular Hydrogel Hybrid as a Fluorescence Sensing Material for Polyanions of Biological Significance, *J. Am. Chem. Soc*., 2009, **13**, 15321-15330.

16. T. Yoshii, S. Onogi, H. Shigemitsu and I. Hamachi, Chemically Reactive Supramolecular Hydrogel Coupled with a Signal Amplification System for Enhanced Analyte Sensitivity, *J. Am. Chem. Soc*., 2015, **137**, 3360-3365.

17. M. A. Ramin, L. Latxague, K. R. Sindhu, O. Chassande and P. Barthélémy, Low molecular weight hydrogels derived from urea based-bolaamphiphiles as new injectable biomaterials, *Biomaterials*, 2017, **145**, 72-80.

18. N. Mizoshita and T. Seki, Organised structures of flexible bolaamphiphiles with trisiloxane spacers: three- and two-dimensional molecular assemblies with different molecular conformation, *Soft Matter*, 2006, **2**, 157–165.

19. Y. Yan, W. Xiong, J. Huang, Z. Li, X. Li, N. Li and H. Fu, Organized Assemblies in Bolaamphiphile/Oppositely Charged Conventional Surfactant Mixed Systems, *J. Phys. Chem. B*., 2005, **109**, 357–364.

20. T. Wang, J. Jiang, Y. Liu, Z. Li and M. Liu, Hierarchical Self-Assembly of Bolaamphiphiles with a Hybrid Spacer and L-Glutamic Acid Headgroup: pH- and Surface-Triggered Hydrogels, Vesicles, Nanofibers, and Nanotubes, *Langmuir,* 2010, **26**, 18694–18700.

21. P. Dhasaiyan and B. L. V. Prasad, Self-Assembly of Bolaamphiphilic Molecules, *Chem. Rev*. 2017, **17**, 597–610.

22. T. Shimizu, R. Iwaura, M. Masuda, T. Hanada and K. Yase, Internucleobase-Interaction-Directed Self-Assembly of Nanofibers from Homo- and Heteroditopic 1,ω-Nucleobase Bolaamphiphiles, *J. Am. Chem. Soc*. 2001, **123**, 5947–5955.

23. T. Wang, Y. Li and M. Liu, Gelation and self-assembly of glutamate bolaamphiphiles with hybrid linkers: effect of the aromatic ring and alkyl spacers, *Soft Matter*, 2009, **5**, 1066–1073.

24. Sudipta Ray, Apurba K. Das, and Arindam Banerjee, pH-Responsive, Bolaamphiphile-Based Smart Metallo-Hydrogels as Potential Dye-Adsorbing Agents, Water Purifier, and Vitamin B12 Carrier, *Chem. Mater*. 2007, **19**, 1633-1639.

25. R.V. Ulijn and A.M. Smith, Designing peptide based nanomaterials, *Chem. Soc. Rev*., 2008, **37**, 664-675.

26. L. A. Estroff and A. D. Hamilton, Water Gelation by Small Organic Molecules, *Chem. Rev*., 2004, **104**, 1201–1218.

27. R. Iwaura, K. Yoshida, M. Masuda, M. Ohnishi-Kameyama, M. Yoshida and T. Shimizu, Oligonucleotide-Templated Self-Assembly of Nucleotide Bolaamphiphiles: DNA-Like Nanofibers Edged by a Double-Helical Arrangement of A–T Base Pairs, *Angew. Chem. Int. Ed. Engl*., 2003, 421009–421012.

28. B. Escuder, S. Martı´ and J. F. Miravet, Organogel Formation by Coaggregation of Adaptable Amidocarbamates and Their Tetraamide Analogues, *Langmuir*, 2005, 216776–216787.

29. X. Guo, D. Xu, H. Yuan, Q. Luo, S. Tang, L. Liu and Y. Wu, A novel fluorescent nanocellulosic hydrogel based on carbon dots for efficient adsorption and sensitive sensing in heavy metals, *J. Mater. Chem. A*, 2019, **7**, 27081–27088.

30. A. Cayuela, M.L. Soriano, S.R. Kennedy, J.W. Steed and M. Valcárcel, Fluorescent carbon quantum dot hydrogels for direct determination of silver ions, *Talanta*, 2016, **151**, 100–105.

31. D.M. Quinn, Acetylcholinesterase: enzyme structure, reaction dynamics, and virtual transition states, *Chem. Rev*., 1987, **87**, 955-979.

32. R. B. Raffa, S. M. Rawls and E. P. Beyzarov, Netter's Illustrated Pharmacology Elsevier; 2014¸ Saunders.

33. R. J. Peiris-John and R. Wickremasinghe, Impact of low-level exposure to organophosphates on human reproduction and survival, *Trans. R. Soc. Trop. Med. Hyg.*, 2008, **102**, 239-245.

34. L. A. Smit, B. N. van-Wendel-de-Joode, D. Heederik, R. J. Peiris-John and W. van der Hoek, Neurological symptoms among Sri Lankan farmers occupationally exposed to acetylcholinesterase-inhibiting insecticides, *Am. J. Ind. Med.*, 2003, **44**, 254-264.

35. R. J. Peiris-John, D. K. Ruberu, A. R. Wickremasinghe, L. A. M. Smit and W. van der Hoek, Effects of Occupational Exposure to Organophosphate Pesticides on Nerve and Neuromuscular Function, *J. Occup. Environ. Med.*, 2002, **44**, 352-357.

36. R. J. Peiris-John, D. K. Ruberu, A. R. Wickremasinghe and W. van-der-Hoek, Low-level exposure to organophosphate pesticides leads to restrictive lung dysfunction, *Respir. Med.*, 2005, **99**, 1319-1324.

37. C. Sahub, T. Tuntulani, T. Nhujak and B. Tomapatanaget, Effective biosensor based on graphene quantum dots via enzymatic reaction for directly photoluminescence detection of organophosphate pesticide, *Sens. Actuators, B.:Chem*., 2018, **258**, 88-97.

38. M. Ikeda, T. Tanida, T. Yoshii and I. Hamachi, Rational molecular design of stimulus-responsive supramolecular hydrogels based on dipeptides, *Adv. mater*., 2011, **23**, 2819-22.

39. A. Mahler, M. Reches, M. Rechter, S. Cohen and E. Gazit, Rigid, Self-Assembled Hydrogel Composed of a Modified Aromatic Dipeptide*, Adv. Mater*., 2006, **18**, 1365-1370.

40. P. Dhasaiyan, A. Banerjee, N. Visaveliya and B. L. V. Prasad Influence of the Sophorolipid Molecular Geometry on their Self-Assembled Structures, *Chem. Asian J.* 2013, **8**, 369 – 372.

41. J.A. Foster, K.K. Damodaran, A. Maurin, G.M. Day, H.P.G. Thompson, G.J. Cameron, J. C. Bernalc and J. W. Steed, Pharmaceutical polymorph control in a drug-mimetic supramolecular gel, *Chem. Sci*., 2017, **8**, 78-84.

42. A. Cayuela, S.R. Kennedy, M.L. Soriano, C.D. Jones, M. Valcárcel and J.W. Steed, Fluorescent carbon dot–molecular salt hydrogels, *Chem. Sci*., 2015, **6**, 6139-6146.

43. N.M. Sangeetha and U. Maitra, Supramolecular gels: functions and uses, *Chem. Soc. Rev*., 2005, **34**, 821-836.

44. A. Kondyurin, I. Levchenko, Z.J. Han, S. Yick, A. Mai-Prochnow, J. Fang, K. Ostrikov, M.M.M. Bilek, Hybrid graphite film–carbon nanotube platform for enzyme immobilization and protection, *Carbo*n, 2013, **65**, 287-295.

45. S. Heinemann, H. Ehrlich, T. Douglas, C. Heinemann, H. Worch, W. Schatton and T. Hanke, Ultrastructural Studies on the Collagen of the Marine Sponge Chondrosia reniformis Nardo, *Biomacromolecules*, 2007, **8**, 3452-3457.

46. A. Barth, Infrared spectroscopy of proteins, *Biochim. Biophys. Acta*, 2007, **1767**, 1073–1101.

47. Y. Dong, J. Shao, C. Chen, H. Li, R. Wang, Y. Chi, X. Lin, G. Chen, Blue luminescent graphene quantum dots and graphene oxide prepared by tuning the carbonization degree of citric acid, *Carbon*, 2012, **50**, 4738-4743.

48. A. Stergioua, R. Cantón-Vitoria, M. N. Psarrou, S. P. Economopoulos, and N. Tagmatarchis, Functionalized graphene and targeted applications – Highlighting the road from chemistry to applications, *Prog. Mater Sci*., 2020, **114**, 100683-100699.

49. F. Chai, T. Wang, L. Li, H. Liu, L. Zhang, Z. Su and C. Wang, Fluorescent gold nanoprobes for the sensitive and selective detection for Hg, *Nanoscale res. lett*., 2010, **5**, 1856-1860.

50. S.R. Lee, H.E. Lee, Y.O. Kang, W.S. Hwang and S.H. Choi, Bienzymatic acetylcholinesterase and choline oxidase immobilized biosensor based on a phenyl carboxylic acid-grafted multiwalled carbon nanotube, *Adv. Mater. Sci. Eng*., 2014, 1-12.

51. S. Ikuta, S. Imamura, H. Misaki and Y. Horiuti, Purification and characterization of choline oxidase from arthrobacter globiformis, *J. Biochem*., 1977, **82**, 1741-1749.

52. L. Yotova and N. Medhat, Co-immobilization of acetylcholinesterase and choline oxidase on new nanohybrid membranes obtained by sol gel technology*, Biotechnol. Biotechnol. Equip*., 2014, **26**, 3039-3043.

53. Z. Zhang, X. Wang and X. Yang, A sensitive choline biosensor using Fe_3O_4 magnetic nanoparticles as peroxidase mimics, *Analyst*, 2011, **136**, 4960-4965.

54. T.D. Lazarević-Pašti, A.M. Bondžić, I.A. Pašti and V.M. Vasić, Indirect electrochemical oxidation of organophosphorous pesticides for efficient detection via acetylcholinesterase test, *Pestic. Biochem. Physiol*., 2012, **104**, 236-242.

55. R. Pimsen, A. Khumsri, S. Wacharasindhu, G. Tumcharern, M. Sukwattanasinitt, Colorimetric detection of dichlorvos using polydiacetylene vesicles with acetylcholinesterase and cationic surfactants, *Biosens. Bioelectron*., 2014, **62**, 8-12.

56. P. Skládal, G.S. Nunes, H. Yamanaka, M.L. Ribeiro, Detection of carbamate pesticides in vegetable samples using cholinesterase-based biosensors, *Electroanalysis*, 1997, **9**, 1083-1087.

57. A.T. Lawal and S.B. Adeloju, Comparison of enzyme immobilisation methods for potentiometric phosphate biosensors, *Biosens. Bioelectron*., 2009, **25**, 406-410.

58. X. Guo, X. Zhang, Q. Cai, T. Shen and S. Zhu, Developing a novel sensitive visual screening card for rapid detection of pesticide residues in food, *Food Control*, 2013, **30**, 15-23.

59. F.C. Wong, M. Ahmad, L.Y. Heng and L.B. Peng, An optical biosensor for dichlovos using stacked sol-gel films containing acetylcholinesterase and a lipophilic chromoionophore, *Talanta*, 2006, **69**, 888-893.

60. A. Mulchandani, S. Pan and W. Chen, Fiber-Optic Enzyme Biosensor for Direct Determination of Organophosphate Nerve Agents, *Biotechnol. Progr*., 1999, **15**, 130-134.

61. L. Qiu, P. Lv, C. Zhao, X. Feng, G. Fang, J. Liu and S. Wang, Electrochemical detection of organophosphorus pesticides based on amino acids conjugated nanoenzyme modified electrodes, *Sens. Actuators, B.:Chem*, 2019, **28**, 6386-6393.

62. I. Walz and W. Schwack, Cutinase inhibition by means of insecticidal organophosphates and carbamates Part 2: screening of representative insecticides on cutinase activity, *Eur. Food Res. Technol*., 2007, **226**, 1135-1143.

63. C. Sicard, C. Glen, B. Aubie, D. Wallace, S. Jahanshahi-Anbuhi, K. Pennings, G.T. Daigger, R. Pelton, J. D. Brennan and C.D. Filipe, Tools for water quality monitoring and mapping using paper-based sensors and cell phones. *Water res*., 2015, **70**, 360-369.

64. https://worldwide.promega.com/resources/guides/lab-equipment-and-supplies/buffers-for-biochemical-reactions/

65. C. M. H. Ferreira, I. S. S. Pinto, E. V. Soares and H. M. V. M. Soares, (Un)suitability of the use of pH buffers in biological, biochemical and environmental studies and their interaction with metal ions – a review, *RSC Adv.*, 2015, **5**, 30989-31003.

66. A. Salis, and M. Monduzzi, Not only pH. Specific buffer effects in biological systems, *Curr. Opin. Colloid. Interface Sci*., 2016, **23**, 1–9.